

Sympathetic nerve damage and restoration after ischemia-reperfusion injury as assessed by ^{11}C -hydroxyephedrine

Rudolf A. Werner^{1,2} · Yoshifumi Maya^{1,3} · Christoph Rischpler⁴ · Mehrbod S. Javadi⁵ · Kazuhito Fukushima⁶ · Constantin Lapa¹ · Ken Herrmann^{1,7} · Takahiro Higuchi^{1,2}

Abstract

Purpose An altered state of the cardiac sympathetic nerves is an important prognostic factor in patients with coronary artery disease. The aim of this study was to investigate regional sympathetic nerve damage and restoration utilizing a rat model of myocardial transient ischemia and a catecholamine analog PET tracer, ^{11}C -hydroxyephedrine (^{11}C -HED).

Methods Transient myocardial ischemia was induced by coronary occlusion for 20 min and reperfusion in male Wistar rats. Dual-tracer autoradiography was performed subacutely (7 days) and chronically (2 months) after ischemia, and in control rats without ischemia using ^{11}C -HED as a marker of sympathetic innervation and ^{201}Tl for perfusion. Additional serial in vivo cardiac ^{11}C -HED and ^{18}F -FDG PET scans were performed in the subacute and chronic phases after ischemia.

Results After transient ischemia, the ^{11}C -HED uptake defect areas in both the subacute and chronic phases were clearly larger than the perfusion defect areas in the midventricular wall. The subacute ^{11}C -HED uptake defect showed a transmural pattern, whereas uptake recovered in the subepicardial portion in the chronic phase. Tyrosine hydroxylase antibody nerve staining confirmed regional denervation corresponding to areas of decreased ^{11}C -HED uptake. Serial in vivo PET imaging visualized reductions in the area of the ^{11}C -HED uptake defects in the chronic phase consistent with autoradiography and histology.

Conclusion Higher susceptibility of sympathetic neurons compared to myocytes was confirmed by a larger ^{11}C -HED defect with a corresponding histologically identified region of denervation. Furthermore, partial reinnervation was observed in the chronic phase as shown by recovery of subepicardial ^{11}C -HED uptake.

✉ Takahiro Higuchi
thiguchi@me.com

Rudolf A. Werner
werner_r1@ukw.de

Keywords ^{11}C -Hydroxyephedrine · Sympathetic nerve · Nerve sprout · Ischemia · Rat

Introduction

Assessment of myocardial sympathetic denervation utilizing radionuclide norepinephrine analog tracers such as ^{11}C -hydroxyephedrine (^{11}C -HED) and ^{123}I -meta-iodobenzylguanidine (^{123}I -MIBG) has emerged as one of the most promising techniques for risk stratification for sudden cardiac death in patients with heart failure and ischemic cardiomyopathy [1–3]. In the most recent clinical trial called PAREPET, ^{11}C -HED PET was used for identifying local cardiac sympathetic nerve damage, and demonstrated independent prognostic value in predicting a high risk of sudden cardiac death [3]. This may provide support for the identification

¹ Department of Nuclear Medicine, University of Würzburg, Oberdürrbacher Strasse 6, 97080 Würzburg, Germany

² Comprehensive Heart Failure Center, University of Würzburg, Oberdürrbacher Strasse 6, 97080 Würzburg, Germany

³ Research Centre, Nihon Medi-Physics Co., Ltd., Chiba, Japan

⁴ Department of Nuclear Medicine, Klinikum rechts der Isar, Technische Universität München, München, Germany

⁵ Division of Nuclear Medicine, Russell H. Morgan Department of Radiology, Johns Hopkins University, Baltimore, MD, USA

⁶ Department of Radiology, Hyogo College of Medicine, Hyogo, Japan

⁷ Department of Molecular and Medical Pharmacology, David Geffen School of Medicine at UCLA, Los Angeles, CA, USA

of heart failure patients most likely to benefit from an implantable cardiac defibrillator, since left ventricular ejection fraction alone is not yet sufficient to identify appropriate candidates [4, 5].

The cardiac sympathetic nerve system is known to be more sensitive to ischemic insult than cardiac myocytes. In animal experimental studies, temporal damage to the cardiac sympathetic nerves after transient ischemia has been shown [6–13]. In humans, several imaging studies using radiolabeled norepinephrine analog tracers have confirmed sympathetic nerve alterations, which are correlated with the area of ischemia in acute coronary syndrome [14]. In the present investigation, in order to improve the understanding of regional and temporal changes in the condition of the sympathetic nerves after transient ischemic injury, we used a well-established rat model of left coronary occlusion and reperfusion [15, 16]. We studied this model with the radionuclide PET tracer ^{11}C -HED [17, 18].

Materials and methods

Animal experiments in a rat model of ischemia (12 animals) and healthy control rats (6 animals) were conducted using ^{11}C -HED and ^{201}Tl dual-tracer autoradiography. Additionally, two rats underwent three in vivo PET sessions before ischemia, and in the subacute and chronic phases of ischemia (Fig. 1). Animal protocols were approved by the local institutional animal care and use committee and were conducted according to the Guide for the Care and Use of Laboratory Animals.

Radiopharmaceuticals

^{11}C -HED was synthesized as previously described [19] and showed specific radioactivities of $> 6 \text{ GBq}/\mu\text{mol}$ and radiochemical purity of $>98 \%$. ^{201}Tl was purchased from GE

Healthcare. ^{18}F -FDG was synthesized in our in-house cyclotron according to the manufacturer's instructions.

Animal model of transient myocardial ischemia

For our experiments male Wistar rats (Charles River Laboratories) were used. Transient myocardial ischemia was performed as previously described [20, 21]. Under general anesthesia with 2 % isoflurane, ischemia was induced by ligating the left coronary artery with a 7-0 polypropylene suture for 20 min via a left lateral thoracotomy. Reperfusion was accomplished by releasing the ligature. The success of coronary occlusion and reperfusion was verified visually by regional cyanosis and blush of the myocardial surface. After closure of their chest, the animals were allowed to recover with appropriate pain medication for postoperative analgesia.

Dual-tracer autoradiography study

Dual-tracer autoradiography of the left ventricular short-axis slices was performed to assess both ^{11}C -HED uptake for sympathetic innervation and ^{201}Tl uptake for reference perfusion. Three groups of animals were studied: (1) subacute phase (day 7 after ischemia, five animals), (2) chronic phase (2 months after ischemia, six animals), and (3) healthy control rats without ischemia (six animals). Both ^{11}C -HED (74 MBq) and ^{201}Tl (0.74 MBq) were injected via a tail vein 20 min and 5 min before the rats were killed. The heart was then extracted, frozen and cut into 20- μm short axis slices using a cryostat. Immediately afterwards, the autoradiography plate (MultiSensitive phosphor screen; PerkinElmer) was first exposed to the slices for 45 min for visualization of ^{11}C -HED distribution with a digital autoradiography system (CR 35 Bio, Raytest or Cyclone; Packard). After 12 h to allow complete decay of ^{11}C , a second exposure to visualize ^{201}Tl distribution was continued for 1 week [17].

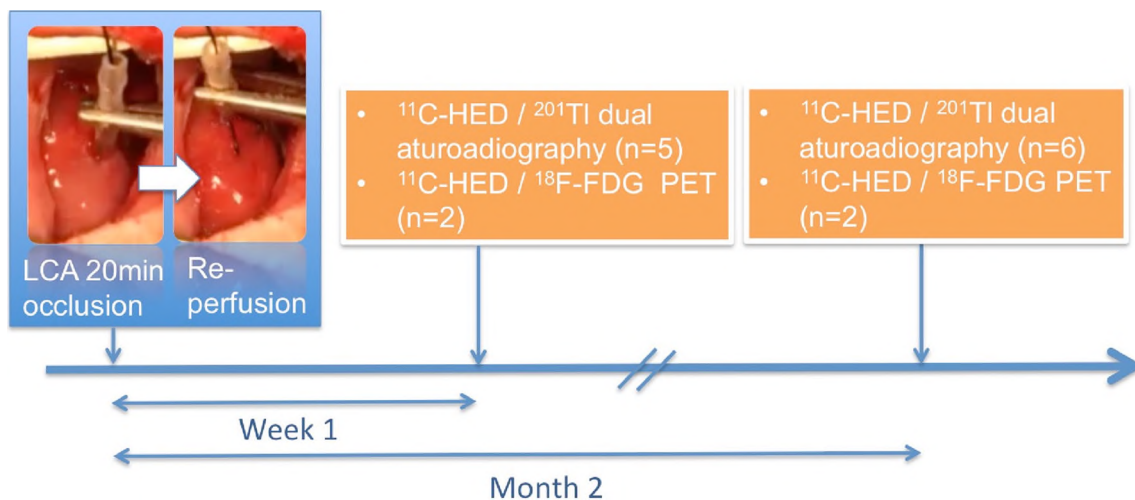
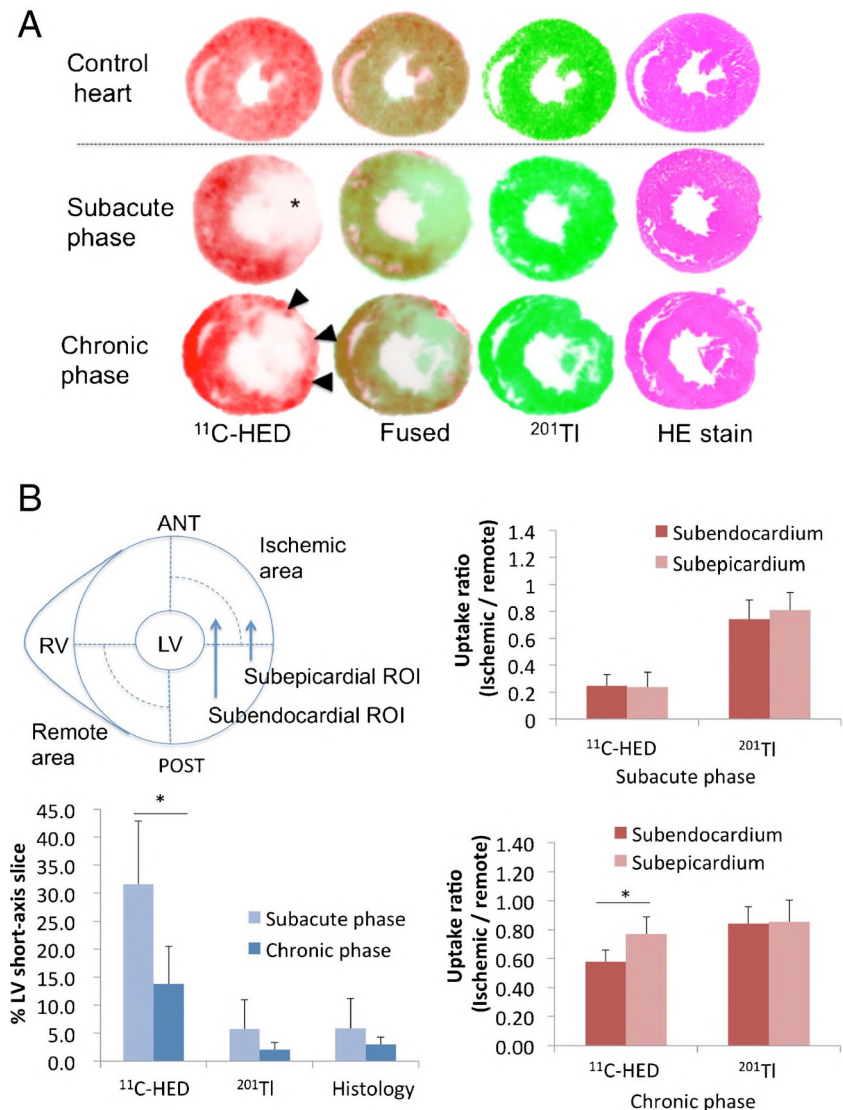


Fig. 1 Schematic diagram illustrating the protocol for the rat model of ischemia (LCA left coronary artery)

In order to quantify tracer uptake distribution, regions of interest (ROIs) were drawn on the anterolateral area at risk of ischemia (25 % of circumference) and a remote control region (opposite 25 % of circumference) on a midmyocardial short-axis section. In order to assess the transmural pattern of tracer distribution in the ventricular wall, the ROIs were divided into subepicardial (inner half) and subendocardial (outer half) wall portions on the slices (Fig. 2). Areas of tracer uptake defect were determined using a threshold of 50 % of maximum myocardial activity on a midventricular short axis slice. Then the uptake defect areas were calculated as percentages in relation to the area of the left ventricular short-axis slice. After autoradiographic exposure, the short axis tissue slices were stained with hematoxylin and eosin (HE) using a standard procedure. The infarct scar area was determined using manual planimetric measurement of the HE staining on digitized photographs.

Histological tissue analysis of the nerve was performed with 7- μm slices adjacent to the cross-sectional left ventricular short-axis slices used for autoradiography analysis. Immunofluorescence staining of catecholaminergic neurons using standard techniques and commercially available rabbit polyclonal ab6211 tyrosine hydroxylase (TH) antibodies (Abcam) was performed. Digitized images were obtained using a fluorescence microscope (model BZ-9000; Keyence) with standardized illumination and contrast. To quantify the percentage of the area with positive TH staining, three fields were randomly selected from ^{11}C -HED uptake-positive and uptake-negative areas on autoradiographic images. The average percentage positive area from the fields was then calculated using BZ-II analyzer software by adjusting the fluorescence intensity threshold of the software so that the visually identified nerve fibers were appropriately selected as closely as possible.

Fig. 2 **a** Representative cross-sectional short-axis images at the midventricular level on dual-tracer autoradiography with ^{11}C -HED and ^{201}Tl after transient coronary occlusion and reperfusion. The area of the transmural ^{11}C -HED defect (*asterisk*) is larger than that of the ^{201}Tl defect 1 week after ischemia. In contrast, the nontransmural ^{11}C -HED uptake defect shows restored uptake at the subepicardial lesion (*arrowheads*) in the chronic phase. **b** Graphs indicate the tracer defect area as a percentage of the left ventricular short-axis slice and the average tracer uptake ratios. The area of the ^{11}C -HED uptake defect was significantly smaller in the chronic phase than in the subacute phase ($*p < 0.01$). ^{11}C -HED uptake in the subepicardial portion is significantly higher than in subendocardial portion in the ischemic area in chronic phase ($*p < 0.01$). ANT anterior wall, POST posterior wall, RV right ventricle, LV left ventricle, ROI region of interest



In vivo PET imaging

A dedicated microPET scanner (Inveon: Siemens) was used to perform serial in vivo cardiac ^{11}C -HED and ^{18}F -FDG PET scans both 1 week and 2 months after myocardial ischemia (two animals). Initially, 10 min after intravenous injection of 37 MBq ^{11}C -HED, static images were acquired over 20 min. As a reference, a second scan with ^{18}F -FDG was performed after more than four half-lives of ^{11}C decay. Starting 60 min after intravenous administration of 37 MBq of ^{18}F -FDG, static PET images were acquired over 15 min.

Statistical analysis

Results are presented as means \pm SD. The two-tailed paired Student's *t* test was used to compare differences between two dependent groups and the two-tailed independent Student's *t* test between independent groups. Values of $p < 0.05$ were considered statistically significant.

Results

Dual-tracer autoradiography

In dual-tracer autoradiography, both ^{11}C -HED and ^{201}Tl were distributed throughout the healthy myocardium of the left ventricle (Fig. 2). After transient ischemia, the area of reduced ^{11}C -HED uptake was found to be larger than the ^{201}Tl defect area in both the subacute and chronic phases after ischemia. The ^{11}C -HED defect area in the left ventricular short-axis slices in the subacute phase ($31.7 \pm 11.2\%$) was significantly larger than in the chronic phase ($13.8 \pm 6.7\%$, $p < 0.01$). The ^{201}Tl uptake defect areas in both the subacute and chronic phases ($5.7 \pm 5.2\%$ and $2.1 \pm 1.2\%$, respectively) were significantly smaller than the ^{11}C -HED defect area ($p < 0.01$ and $p < 0.05$, respectively). There were no significant differences between the ^{201}Tl uptake defect areas and the scar areas identified on HE staining (scar areas $5.8 \pm 5.4\%$ and $3.0 \pm 1.3\%$ in the subacute and chronic phases, respectively). Interestingly, the transmural pattern of the ^{11}C -HED defect was different between the subacute and chronic phases. The defect was transmural in the subacute phase and ^{11}C -HED activity in the subepicardium was restored in the chronic phase. ^{11}C -HED uptake ratios (vs. the remote control region) in the subendocardial and subepicardial portions were 0.25 ± 0.08 and 0.24 ± 0.11 (not significantly different) in the subacute phase, and 0.58 ± 0.08 and 0.77 ± 0.12 ($p < 0.01$) in the chronic phase, respectively. On the other hand, the ^{201}Tl uptake ratios - positive fibers was well matched with the area of ^{11}C -HED uptake in both the subacute and chronic phases (Fig. 3). TH-immunopositive nerve densities in the ^{11}C -HED-positive and ^{11}C -HED-negative areas were significantly different in both

the subacute phase ($0.51 \pm 0.27\%$ vs. $0.15 \pm 0.11\%$, $p < 0.05$) and the chronic phase ($0.67 \pm 0.20\%$ vs. $0.07 \pm 0.08\%$, $p < 0.01$).

In vivo PET imaging

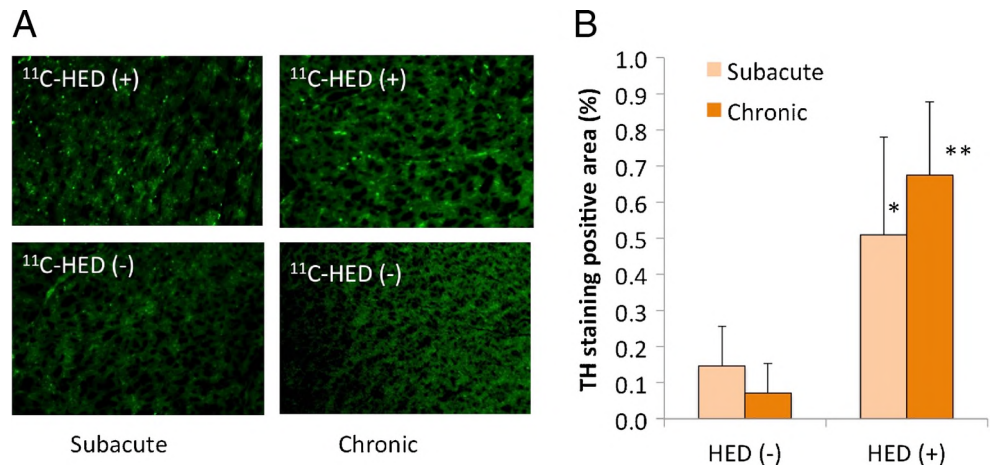
In vivo PET imaging visualized the ^{11}C -HED defect corresponding to the ex vivo autoradiographic findings after ischemia. ^{18}F -FDG uptake was preserved throughout the ventricle, indicating preserved myocardial viability at the ^{11}C -HED defect area. Furthermore, the reduction in the ^{11}C -HED defect area in the chronic phase after ischemia was confirmed on serial imaging (Fig. 4).

Discussion

The present study investigated regional patterns of sympathetic nerve degradation and restoration utilizing the radionuclide PET tracer ^{11}C -HED after 20 min of transient ischemia in a rat model. Transmural ^{11}C -HED uptake defects in the subacute phase and partial subepicardial recovery of ^{11}C -HED uptake in the chronic phase were visualized autoradiographically. These regional ^{11}C -HED uptake findings showed a close correlation with sympathetic denervation as determined by TH immunofluorescence staining. Furthermore, using dual-tracer autoradiography, preserved uptake of ^{201}Tl in the ^{11}C -HED defect areas confirmed myocardial viability and excluded abnormalities of myocardial perfusion as a cause of decreased ^{11}C -HED uptake. Additionally, in vivo serial PET imaging visualized the changes in the ^{11}C -HED defect noninvasively. To the best of our knowledge, this is the first demonstration of ^{11}C -HED distribution patterns in histologically confirmed areas of denervation and reinnervation of the heart after transient ischemia.

^{11}C -HED is one of the most widely used PET tracers for determining the innervation in the heart. High affinity for the norepinephrine transporter is well characterized in several species including rodents and humans [17, 20]. Although rats are commonly used animals for studying cardiac diseases, there are significant differences in myocardial norepinephrine handling between rats and humans. In addition to the common reuptake mechanism transporting norepinephrine at the nerve terminal (uptake 1), the nonneural uptake system (uptake 2) plays an important role in the rat heart. This mechanism transports norepinephrine into the myocytes and this is followed by enzymatic degradation, which is not considered to be relevant in the human heart. To fully characterize the sympathetic nerve system, the specific properties of commonly used norepinephrine analog tracers related to animal models must be taken into consideration. The specificity of the two most commonly used clinical radiolabeled nerve tracers, ^{123}I -MIBG and ^{11}C -HED, have been tested in rat hearts [17]. Cardiac ^{11}C -

Fig. 3 **a** Representative images showing tyrosine hydroxylase immunofluorescence staining in the ^{11}C -HED defect area (*HED* (-)) and a remote control area (*HED* (+)) in the left ventricular wall in the subacute and chronic phases after transient ischemia in a rat model. **b** There is an extensive reduction in TH-positive cells in ^{11}C -HED defect areas in both the subacute and chronic phases after ischemia (* $p < 0.05$, ** $p < 0.01$, vs. *HED* (-))



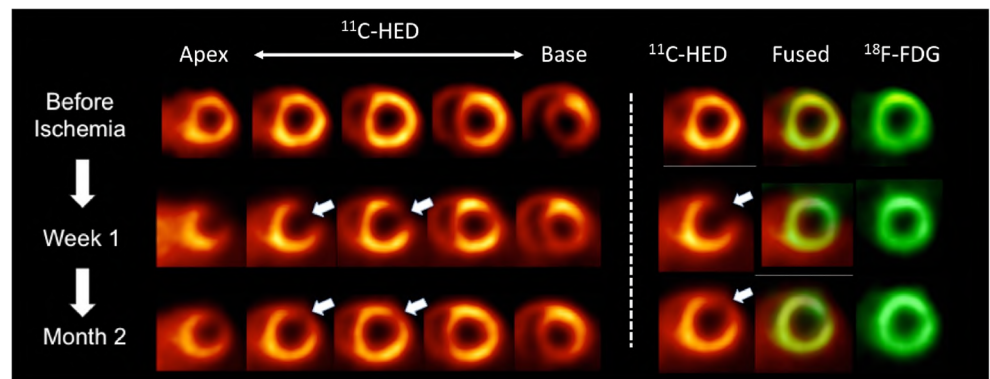
HED uptake showed very high specificity for neural uptake 1, which was confirmed by desipramine blockage of more than 90%. However, ^{123}I -MIBG uptake demonstrated a significant contribution from nonneural uptake 2, which was confirmed by desipramine and phenoxybenzamine (uptake 1 and 2 blockage) blocking studies. Similar results have been reported for the nonneural uptake of the recently introduced ^{18}F -labeled PET tracer, LMI1195, that is similar to MIBG being based on a benzylguanidine structure [21].

It has been reported that myocardial ischemia can cause sympathetic nerve damage that is thought to play a critical role in ventricular arrhythmogenesis [22, 23]. Studies in dogs have shown that a hypoxic environment at the myocardial peri-infarction zone can cause functional denervation with the generation of viable but denervated myocardial tissue [6]. Imaging approaches have confirmed corresponding findings in human hearts. Larger areas of sympathetic neuronal damage measured by ^{123}I -MIBG uptake were well matched to areas of myocardium at risk in patients with acute coronary syndrome after revascularization [14]. A recent clinical trial further indicated the clinical significance of ^{11}C -HED PET-derived denervation as a significant predictor of sudden cardiac death [3]. Denervated myocardial tissue may contribute to the earliest endocardial activation of ventricular

tachycardia, as suggested in pig experimental models of myocardial infarction [24]. We successfully replicated and visualized viable but denervated myocardial tissue in a rat model after 20 min of transient ischemia. Larger ^{11}C -HED defects exceeding the area of the hypoperfused scar were demonstrated with a dual tracer autoradiography assay. Further histological analyses confirmed anatomical denervation corresponding to the area of the ^{11}C -HED defect. These results are in line with previous findings in humans and large animals demonstrating higher susceptibility of nerve cells to ischemic injury than myocytes [14]. It should be noted that the present experimental set-up by utilizing a small-animal model had a number of advantages such as cost-effectiveness, easier handling and higher reproducibility.

Reinnervation of the ischemically denervated tissue in patients with acute coronary syndrome has been suggested but has still not been conclusively shown. In an early experiment with large animals, Minardo et al. confirmed sympathetic reinnervation by complete restoration of ^{123}I -MIBG uptake correlating with electrophysiological responses 14 weeks after myocardial infarction or phenol denervation treatment [25]. In contrast, Fallavollita et al. did not find any change in defect size after revascularization of reversibly ischemic myocardium in swine with hibernating myocardium over 4 weeks using

Fig. 4 In vivo serial PET imaging with ^{11}C -HED and ^{18}F -FDG in a rat model before and after transient ischemia. The regional ^{11}C -HED uptake defect (arrows) with preserved ^{18}F -FDG uptake is seen only after ischemia. The defect in ^{11}C -HED uptake at 1 week is reduced at 2 months



^{11}C -HED PET [26]. In human hearts, slow (after >18 months) but progressive reinnervation has been shown by various approaches including PET imaging in patients after heart transplantation [27]. However, clinical reports of reinnervation of viable but denervated myocardial tissue in patients with ischemic heart disease are very limited and inconsistent.

Allman et al. studied 16 patients with a first acute myocardial infarction who had serial ^{11}C -HED PET and ammonia perfusion imaging performed at 7 days and 8 months, but no change in the ^{11}C -HED abnormalities was observed [13]. On the other hand, Hartikainen et al. studied 13 patients using ^{123}I -MIBG SPECT and perfusion scintigraphy and found partial reinnervation at the peri-infarction zone between 3 and 12 months [12]. The present study using a rat model of transient coronary occlusion and reperfusion confirmed significant anatomical reinnervation and corresponding recovery of ^{11}C -HED uptake in the area at risk. One of the limitations of the present study was the small size of the rodent heart. Further correlative studies using a large-animal model are warranted to provide a better understanding of the dynamics of sympathetic reinnervation in the human heart.

Interestingly, the present results show that the reinnervation was limited to the subepicardial portion of the myocardium. This spatial pattern of reinnervation might be partly explained by the anatomy of sympathetic nerve distribution in the heart. Sympathetic nerve fibers first travel along the surface of the heart accompanying pericardial vascular structures and then penetrate the myocardium from the epicardial side [28]. Therefore, it is plausible that the reinnervation process starts in the epicardium. Furthermore, blocking of sympathetic nerve regeneration by inhibitory components of the extracellular matrix has recently been reported [8]. The presence of endocardial nontransmural scar tissue may be one factor contributing to the inhibition of further nerve growth towards the distal endocardial portion of the ventricle.

We employed only a midventricular slice from each heart for the autoradiographic analysis instead of using multiple slices from the entire heart. Infarct size and defect area expressed as a percentage of the whole left ventricular area cannot be accurately assessed. This is because of the methodological limitation of using a tracer with very short physiological half-life (^{11}C , $T_{1/2}$ 20 min). This requires prompt exposure of the sliced samples before radioactive decay. However, we also note that the difference in radioactive decay of the two tracers in our dual-tracer assay was of value in the analysis. The distribution of ^{201}Tl ($T_{1/2}$ 74 h) could also be analyzed as a reference in exactly same tissue slices, which strengthened the results relating to ^{11}C -HED distribution.

In conclusion, we investigated sympathetic nerve damage and regeneration utilizing a rat model of myocardial transient ischemia and a catecholamine analog PET tracer, ^{11}C -HED. Our results confirmed that sympathetic neurons are more susceptible to ischemic injury than myocytes. Additionally,

reinnervation was shown by differences in the pattern of ^{11}C -HED distribution in the subacute and the chronic phases. This discrepancy in ^{11}C -HED distribution was confirmed by initial transmural denervation in the subacute phase followed by partial subepicardial nerve restoration in the area at risk during the chronic phase.

Compliance with ethical standards

Funding This work was supported by the Competence Network of Heart Failure funded by the Integrated Research and Treatment Center (IFB) of the Federal Ministry of Education and Research (BMBF) and the German Research Council (DFG grant HI 1789/2-1).

Conflicts of interest None.

Ethical approval All applicable international, national, and/or institutional guidelines for the care and use of animals were followed. All procedures performed in studies involving animals were in accordance with the ethical standards of the institution or practice at which the studies were conducted. This article does not describe any studies with human participants performed by any of the authors.

References

1. Al Badarin FJ, Wimmer AP, Kennedy KF, Jacobson AF, Bateman TM. The utility of ADMIRE-HF risk score in predicting serious arrhythmic events in heart failure patients: incremental prognostic benefit of cardiac ^{123}I -mIBG scintigraphy. *J Nucl Cardiol.* 2014;21:756–62.
2. Sood N, Al Badarin F, Parker M, Pullatt R, Jacobson AF, Bateman TM, et al. Resting perfusion MPI-SPECT combined with cardiac ^{123}I -mIBG sympathetic innervation imaging improves prediction of arrhythmic events in non-ischemic cardiomyopathy patients: sub-study from the ADMIRE-HF trial. *J Nucl Cardiol.* 2013;20: 813–20.
3. Fallavollita JA, Heavey BM, Luisi Jr AJ, Michalek SM, Baldwa S, Mashtare Jr TL, et al. Regional myocardial sympathetic denervation predicts the risk of sudden cardiac arrest in ischemic cardiomyopathy. *J Am Coll Cardiol.* 2014;63:141–9.
4. Moss AJ, Zareba W, Hall WJ, Klein H, Wilber DJ, Cannom DS, et al. Prophylactic implantation of a defibrillator in patients with myocardial infarction and reduced ejection fraction. *N Engl J Med.* 2002;346:877–83.
5. Passman R, Goldberger JJ. Predicting the future: risk stratification for sudden cardiac death in patients with left ventricular dysfunction. *Circulation.* 2012;125:3031–7.
6. Inoue H, Zipes DP. Time course of denervation of efferent sympathetic and vagal nerves after occlusion of the coronary artery in the canine heart. *Circ Res.* 1988;62:1111–20.
7. Abe T, Morgan DA, Gutterman DD. Protective role of nerve growth factor against postischemic dysfunction of sympathetic coronary innervation. *Circulation.* 1997;95:213–20.
8. Gardner RT, Habecker BA. Infarct-derived chondroitin sulfate proteoglycans prevent sympathetic reinnervation after cardiac ischemia-reperfusion injury. *J Neurosci.* 2013;33:7175–83.
9. Lee TM, Lin MS, Chang NC. Effect of pravastatin on sympathetic reinnervation in postinfarcted rats. *Am J Physiol Heart Circ Physiol.* 2007;293:H3617–26.

10. Oh YS, Jong AY, Kim DT, Li H, Wang C, Zemljic-Harpf A, et al. Spatial distribution of nerve sprouting after myocardial infarction in mice. *Heart Rhythm*. 2006;3:728–36.
11. Fallen EL, Coates G, Nahmias C, Chirakal R, Beanlands R, Wahl L, et al. Recovery rates of regional sympathetic reinnervation and myocardial blood flow after acute myocardial infarction. *Am Heart J*. 1999;137:863–9.
12. Hartikainen J, Kuikka J, Mantysaari M, Lansimies E, Pyorala K. Sympathetic reinnervation after acute myocardial infarction. *Am J Cardiol*. 1996;77:5–9.
13. Allman KC, Wieland DM, Muzik O, Degrado TR, Wolfe Jr ER, Schwaiger M. Carbon-11 hydroxyephedrine with positron emission tomography for serial assessment of cardiac adrenergic neuronal function after acute myocardial infarction in humans. *J Am Coll Cardiol*. 1993;22:368–75.
14. Matsunari I, Schricke U, Bengel FM, Haase HU, Barthel P, Schmidt G, et al. Extent of cardiac sympathetic neuronal damage is determined by the area of ischemia in patients with acute coronary syndromes. *Circulation*. 2000;101:2579–85.
15. Higuchi T, Fukushima K, Xia J, Mathews WB, Lautamaki R, Bravo PE, et al. Radionuclide imaging of angiotensin II type 1 receptor upregulation after myocardial ischemia-reperfusion injury. *J Nucl Med*. 2010;51:1956–61.
16. Higuchi T, Nekolla SG, Huisman MM, Reder S, Poethko T, Yu M, et al. A new 18F-labeled myocardial PET tracer: myocardial uptake after permanent and transient coronary occlusion in rats. *J Nucl Med*. 2008;49:1715–22.
17. Rischpler C, Fukushima K, Isoda T, Javadi MS, Dannals RF, Abraham R, et al. Discrepant uptake of the radiolabeled norepinephrine analogues hydroxyephedrine (HED) and metaiodobenzylguanidine (MIBG) in rat hearts. *Eur J Nucl Med Mol Imaging*. 2013;40:1077–83.
18. Higuchi T, Schwaiger M. Imaging cardiac neuronal function and dysfunction. *Curr Cardiol Rep*. 2006;8:131–8.
19. Rosenspire KC, Haka MS, Van Dort ME, Jewett DM, Gildersleeve DL, Schwaiger M, et al. Synthesis and preliminary evaluation of carbon-11-meta-hydroxyephedrine: a false transmitter agent for heart neuronal imaging. *J Nucl Med*. 1990;31:1328–34.
20. Munch G, Nguyen NT, Nekolla S, Ziegler S, Muzik O, Chakraborty P, et al. Evaluation of sympathetic nerve terminals with [(11)C]epinephrine and [(11)C]hydroxyephedrine and positron emission tomography. *Circulation*. 2000;101:516–23.
21. Higuchi T, Yousefi BH, Kaiser F, Gartner F, Rischpler C, Reder S, et al. Assessment of the 18F-labeled PET tracer LMI1195 for imaging norepinephrine handling in rat hearts. *J Nucl Med*. 2013;54:1142–6.
22. Zipes DP, Rubart M. Neural modulation of cardiac arrhythmias and sudden cardiac death. *Heart Rhythm*. 2006;3:108–13.
23. Lautamaki R, Sasano T, Higuchi T, Nekolla SG, Lardo AC, Holt DP, et al. Multiparametric molecular imaging provides mechanistic insights into sympathetic innervation impairment in the viable infarct border zone. *J Nucl Med*. 2015;56:457–63.
24. Sasano T, Abraham MR, Chang KC, Ashikaga H, Mills KJ, Holt DP, et al. Abnormal sympathetic innervation of viable myocardium and the substrate of ventricular tachycardia after myocardial infarction. *J Am Coll Cardiol*. 2008;51:2266–75.
25. Minardo JD, Tuli MM, Mock BH, Weiner RE, Pride HP, Wellman HN, et al. Scintigraphic and electrophysiological evidence of canine myocardial sympathetic denervation and reinnervation produced by myocardial infarction or phenol application. *Circulation*. 1988;78:1008–19.
26. Fallavollita JA, Banas MD, Suzuki G, deKemp RA, Sajjad M, Cauty Jr JM. 11C-meta-hydroxyephedrine defects persist despite functional improvement in hibernating myocardium. *J Nucl Cardiol*. 2010;17:85–96.
27. Bengel FM, Ueberfuhr P, Ziegler SI, Nekolla S, Reichart B, Schwaiger M. Serial assessment of sympathetic reinnervation after orthotopic heart transplantation. A longitudinal study using PET and C-11 hydroxyephedrine. *Circulation*. 1999;99:1866–71.
28. Ieda M, Kanazawa H, Kimura K, Hattori F, Ieda Y, Taniguchi M, et al. *Sema3a* maintains normal heart rhythm through sympathetic innervation patterning. *Nat Med*. 2007;13:604–12.